J|A|C|S ARTICLES

Published on Web 08/23/2010

Self-Assembly of Supramolecular Fullerene Ribbons via Hydrogen-Bonding Interactions and Their Impact on Fullerene Electronic Interactions and Charge Carrier Mobility

Cheng-Che Chu,[†] Guillaume Raffy,[†] Debdas Ray,[†] André Del Guerzo,[†] Brice Kauffmann,[‡] Guillaume Wantz,[§] Lionel Hirsch,[§] and Dario M. Bassani*[,†]

Institut des Sciences Moléculaires, CNRS UMR 5255, Université Bordeaux 1, 351, Cours de la Libération, 33405 Talence, France, Institut Européen de Chimie et Biologie, UMS 3033 CNRS, Université de Bordeaux, 2 rue Robert Escarpit, 33607 Pessac, France, and Laboratoire d'Intégration des Matériaux aux Systèmes, CNRS UMR 5218, Université de Bordeaux, Institut Polytechnique de Bordeaux, ENSCBP, 16 Av. Pey Berland, 33607 Pessac, France

Received June 1, 2010; E-mail: d.bassani@ism.u-bordeaux1.fr

Abstract: The anisotropy of the electronic interactions between fullerenes in crystalline solids was examined using a confocal fluorescence microscope by probing the polarization of the fluorescence emission arising from fullerene excimer-like emitting states. Crystals of C_{60} obtained by vacuum-sublimation or from chloroform solution exhibited no or little polarization ($p = 0$ or 0.11, respectively), as expected from the high symmetry of the C_{60} fcc lattice or the low degree of anisotropy induced by included solvent molecules. The use of hydrogen-bonding to supramolecularly control interfullerene electronic interactions was explored using a fullerene derivative (**1**) combining a solubilizing 3,4-di-*tert*-butylbenzene group and a barbituric acid hydrogen-bonding (H-B) moiety. The crystal structure of **1** establishes the existence of fullerene H-B tapes along which interfullerene electronic interactions are expected to be large. In agreement with this, we observe very strong polarization of the fullerene excimer-like emission ($p = 0.78$), indicative of a high degree of anisotropy in the fullerene interactions. The charge-carrier mobility of **1** as determined from OFET devices was found to be lower than that of C_{60} (1.2×10^{-4} vs 1.2×10^{-2} cm^2/s V), which is rationalized on the basis of the reduced dimensionality of **1** as a wire-like semiconductor and variations in the morphology of the device active layer revealed by AFM measurments.

1. Introduction

Besides being a major goal in supramolecular chemistry, designing molecular components possessing the necessary chemical information to self-assemble into well-defined architectures represents a major route toward devising materials with molecular precision that can bridge the gap between top-down and bottom-up engineering while providing improved performance.[1] Compared to other intermolecular forces, such as van der Waals, π-stacking, or Coulombic interactions, hydrogen bonds (H-B) are particularly attractive as they are directional and do not possess electronic energy levels that interfere with those in materials for organic electronics applications.[2] It is no surprise, therefore, that great effort has been expended toward the preparation and characterization of photo- and electro-active noncovalent assemblies based on H-B. However, whereas a variety of electron donors (e.g., porphyrins, oligothiophenes, oligophenylenevinylenes) possessing H-B units have been investigated,[3] the choice of molecular components for *n*-type materials has mostly focused on C_{60} derivatives.[4]

[†] Institut des Sciences Moléculaires.
[‡] Institut Européen de Chimie et Biologie.
[§] Laboratoire d'Intégration des Matériaux aux Systèmes.

(1) (a) Grozema, F. C.; Siebbeles, L. D. A. *Int. Rev. Phys. Chem.* **2008**, *27*, 87. (b) Chu, C. C.; Bassani, D. M. *Photochem. Photobiol. Sci.* **2008**, *7*, 521.

(2) (a) El-Ghayoury, A.; Schenning, A.; van Hal, P. A.; van Duren, J. K. J.; Janssen, R. A. J.; Meijer, E. W. *Angew. Chem., Int. Ed.* **2001**, *40*, 3660. (b) Huang, C. H.; Bassani, D. M. *Eur. J. Org. Chem.* **2005**, 4041.

(3) For representative examples, see: (a) Hoeben, F. J. M.; Pouderoijen, M. J.; Schenning, A.; Meijer, E. W. *Org. Biomol. Chem.* **2006**, *4*, 4460. (b) D'Souza, F.; Venukadasula, G. M.; Yamanaka, K.; Subbaiyan, N. K.; Zandler, M. E.; Ito, O. *Org. Biomol. Chem.* **2009**, *7*, 1076. (c) Chen, Z. J.; Lohr, A.; Saha-Moller, C. R.; Wurthner, F. *Chem. Soc. Rev.* **2009**, *38*, 564. (d) Kang, S. C.; Umeyama, T.; Ueda, M.; Matano, Y.; Hotta, H.; Yoshida, K.; Isoda, S.; Shiro, M.; Imahori, H. *Adv. Mater.* **2006**, *18*, 2549. (e) Imahori, H.; Liu, J. C.; Hotta, H.; Kira, A.; Umeyama, T.; Matano, Y.; Li, G. F.; Ye, S.; Isosomppi, M.; Tkachenko, N. V.; Lemmetyinen, H. *J. Phys. Chem. B* **2005**, *109*, 18465. (f) Yoon, S. M.; Hwang, I. C.; Kim, K. S.; Choi, H. C. *Angew. Chem., Int. Ed.* **2009**, *48*, 2506. (g) Drain, C. M.; Batteas, J. D.; Flynn, G. W.; Milic, T.; Chi, N.; Yablon, D. G.; Sommers, H. *Proc. Natl. Acad. Sci. U.S.A.* **2002**, *99*, 6498. (h) Hu, J. S.; Guo, Y. G.; Liang, H. P.; Wan, L. J.; Jiang, L. *J. Am. Chem. Soc.* **2005**, *127*, 17090. (i) Hill, J. P.; Jin, W. S.; Kosaka, A.; Fukushima, T.; Ichihara, H.; Shimomura, T.; Ito, K.; Hashizume, T.; Ishii, N.; Aida, T. *Science* **2004**, *304*, 1481. (j) Bayard, E.; Hamel, S.; Rochefort, A. *Org. Electron.* **2006**, *7*, 144. (k) Yagai, S.; Monma, Y.; Kawauchi, N.; Karatsu, T.; Kitamura, A. *Org. Lett.* **2007**, *9*, 1137. (l) Hoeben, F. J. M.; Zhang, J.; Lee, C. C.; Pouderoijen, M. J.; Wolffs, M.; Wurthner, F.; Schenning, A.; Meijer, E. W.; De Feyter, S. *Chem.—Eur. J.* **2008**, *14*, 8579. (m) Fang, F. C.; Chu, C. C.; Huang, C. H.; Raffy, G.; Del Guerzo, A.; Wong, K. T.; Bassani, D. M. *Chem. Commun.* **2008**, 6369.

(4) Mallik, A. B.; Locklin, J.; Mannsfeld, S. C. B.; Reese, C.; Roberts, M. S.; Senatore, M. L.; Zi, H.; Bao, Z. In *Organic Field-Effect Transistors*; Bao, Z., Locklin, J., Eds.; CRC Press: Boca Raton, FL, 2007.

 © 2010 American Chemical Society

Since initial reports of fullerene adducts containing H-B moieties,[5] the number of H-B substituted-fullerene derivatives has increased steadily[6,7] Our initial efforts led to a fullerene-barbituric acid adduct that opened up access to a variety of well-defined supramolecular C_{60} architectures,[8] based on the melamine-cyanuric acid motif, that display enhanced electronic properties of interest in organic photovoltaics[9] and for the study of through-space electronic interactions.[10] Despite the strong interest in developing H-B supramolecular fullerene-based materials, there is still no direct evidence as to whether the self-assembly properties of such materials are indeed controlled by the H-B interactions rather than by the strong aggregation properties of fullerene, dominated by entropy loss due to solvation.[11] Furthermore, it is not yet clear whether the presence of H-B units can indeed direct interfullerene electronic interactions, nor to what degree they are compatible with charge transport in *n*-type fullerene-based semiconductors. Herein, we provide experimental evidence for the self-assembly of a H-B fullerene derivative into a one-dimensional tape and its effect on determining the directionality of through-space interfullerene electronic interactions probed using the polarization of the fluorescence emission from fullerene excimer-like emitting states in single crystals. Compared to fullerene nanowires obtained by Langmuir−Blodgett deposition of organogellators,[12] the crystalline materials show very high molecular ordering. Furthermore, we establish that the presence of H-B motifs is compatible with *n*-type charge transport in OFET devices.

2. Experimental Section

2.1. Synthesis of 1. A chlorobenzene solution (200 mL) containing C_{60} (1.223 g, 1.62 mmol) was degassed by three freeze−pump−thaw cycles. The solution was brought to reflux, and azido di-*tert*-butylbenzyl barbiturate (276 mg, 0.81 mmol) in chlorobenzene (this solution was degassed by three cycles of freeze−pump−thaw) was added dropwise. After refluxing for 2 days, the solvent was removed under reduced pressure. The crude product was dry-loaded onto a silica column and washed with toluene to remove C_{60} prior to elution with a mixture of 5% ethyl acetate in toluene to afford the desired product. The solvent was dried under vacuum to afford a brown powder product (0.32 g, yield = 37%). MALDI-MS *m*/*z* (%) 1063.95 ($[M + H]^+$, 83), 1085.98 ($[M + Na]^+$, 100), 1101.93 ($[M + K]^+$, 30), 1314.08 ($[M + DCTB]^+$, 44), 1337.10 ($[M + DCTB + Na]^+$, 20).

2.2. Confocal Fluorescence Microscopy. Measurements were performed on a Picoquant Microtime 200 inverted confocal microscope, using a PicoHarp 300 multichannel single photon counter and two MPD SPADs. The excitation originated from a frequency doubled Ti-Sa laser (Coherent) tuned at 385 nm with picosecond pulses (4−6 ps) at 4.76 MHz repetition rate. The laser beam was injected by 90° reflection on a 80%T/20%R spectrally flat beam splitter into the microscope objective (100× UPLSAPO, N.A. 1.4). Linearly polarized excitation light was obtained with a Babinet Soleil compensator. The emission was collected by transmission through the same beam splitter and a suitable interferential filter before being focused on a 50 μm pinhole. Parallel and perpendicular components of the emitted light were split using a polarizing beam splitter and two Glan-Thompson polarizers. The instrumental *G*-factor is measured on the pertinent spectral range (650−900 nm) using emission from the crystals and the relation $G = (I_{VV}I_{HV}/I_{VH}I_{HH})^{1/2}$, where the indexes H and V refer to the horizontal and vertical position of the excitation (first index) or emission (second index) polarizers, rotating the crystal by 90° around the optical axis when the excitation polarization is changed from V to H. After the pinhole, light can be diverted into an Andor SR300i spectrometer equipped with a Newton EM-CCD for spectroscopy measurements.

2.3. Crystal Structure Determination. Single crystals of **1** were grown by the slow diffusion of chloroform into an *o*-dichlorobenzene solution of **1** and belong to the triclinic space group with cell parameters $C_{79}H_{25}N_3O_3 \cdot CHCl_3$; MW =1183.4, $a = 9.952(2)$ Å, $b = 15.876(3)$ Å, $c = 15.877(3)$ Å, $\alpha = 77.41(3)°$, $\beta = 83.69(3)°$, $\gamma = 88.42(3)°$, $V = 2433(8)$ Å^3, $Z = 2$ and $\rho_{calc} = 1.615$ g Å cm^{-3}. Data were collected at 100(2) K on Proxima1 beamline at a wavelength $\lambda = 0.8550$ Å, with $2\theta_{max} = 26.74°$ using φ scans. 21128 reflections, 5465 independent, R(int) = 0.0416. Data were processed using the XDS package.[13] The positions of non-H atoms were determined by the program SHELXD, and the position of the H atoms were deduced from coordinates of the non-H atoms and confirmed by Fourier synthesis. H atoms were included for structure factor calculations but not refined. The structure was refined using SHELXL.[14] Refinement statistics: goodness-of-fit on $F^2 = 1.657$, final R indices [$I > 2\sigma(I)$], $R1 = 0.1122$, $wR2 = 0.3345$; R indices (all data): $R1 = 0.1250$, $wR2 = 0.3490$. CCDC 742195 contains the supplementary crystallographic data for this paper. These data can be obtained free of charge from The Cambridge Crystallographic Data Centre via www.ccdc.cam.ac.uk/data_request/cif.

2.4. Preparation of OFET Devices. The SiO_2/Si substrates were cleaned in acetone and isopropyl alcohol for 30 min each and transferred to a Jelight Company Inc. UVO Cleaner 42-220 for surface cleaning for 5 min. C_{60} or **1** was thermally evaporated under vacuum (ca. 1×10^{-6} mbar) onto the cleaned SiO_2/Si substrates heated at 44 °C for C_{60} and 57 °C for **1** during evaporation on an Edwards Auto 306 evaporator. Film thicknesses were controlled with a Temcor Alpha Step IQ tactile profilometer. The coated SiO_2/Si substrates were then transferred to an evaporator in a glovebox, and calcium electrodes were deposited by thermal evaporation under vacuum (1×10^{-6} mbar) through a shadow mask to define a round device of 3 mm in diameter possessing a central gap of 25 μm in width. The characterization was carried out using a Keithley 4200

(5) (a) Gonzalez, J. J.; Gonzalez, S.; Priego, E. M.; Luo, C. P.; Guldi, D. M.; de Mendoza, J.; Martin, N. *Chem. Commun.* **2001**, 163. (b) Rispens, M. T.; Sanchez, L.; Knol, J.; Hummelen, J. C. *Chem. Commun.* **2001**, 161. (c) Diederich, F.; Echegoyen, L.; Gomez-Lopez, M.; Kessinger, R.; Stoddart, J. F. *J. Chem. Soc., Perkin Trans. 2* **1999**, 1577.

(6) (a) Shi, Z. Q.; Li, Y. L.; Gong, H. F.; Liu, M. H.; Xiao, S. X.; Liu, H. B.; Li, H. M.; Xiao, S. Q.; Zhu, D. B. *Org. Lett.* **2002**, *4*, 1179. (b) Zhuang, J. P.; Zhou, W. D.; Li, X. F.; Li, Y. J.; Wang, N.; He, X. R.; Liu, H. B.; Li, Y. L.; Jiang, L.; Huang, C. S.; Cui, S.; Wang, S.; Zhu, D. B. *Tetrahedron* **2005**, *61*, 8686. (c) Wessendorf, F.; Gnichwitz, J. F.; Sarova, G. H.; Hager, K.; Hartnagel, U.; Guldi, D. M.; Hirsch, A. *J. Am. Chem. Soc.* **2007**, *129*, 16057. (d) Figueira-Duarte, T. M.; Gegout, A.; Nierengarten, J. F. *Chem. Commun.* **2007**, 109. (e) D'Souza, F.; Gadde, S.; Islam, D. M. S.; Pang, S. C.; Schumacher, A. L.; Zandler, M. E.; Horie, R.; Araki, Y.; Ito, O. *Chem. Commun.* **2007**, 480. (f) Sanchez, L.; Rispens, M. T.; Hummelen, J. C. *Angew. Chem., Int. Ed.* **2002**, *41*, 838. (g) Eckert, J. F.; Nicoud, J. F.; Nierengarten, J. F.; Liu, S. G.; Echegoyen, L.; Barigelletti, F.; Armaroli, N.; Ouali, L.; Krasnikov, V.; Hadziioannou, G. *J. Am. Chem. Soc.* **2000**, *122*, 7467. (h) Sary, N.; Richard, F.; Brochon, C.; Leclerc, N.; Leveque, P.; Audinot, J. N.; Berson, S.; Heiser, T.; Hadziioannou, G.; Mezzenga, R. *Adv. Mater.* **2010**, *22*, 763.

(7) For a review of supramolecular fullerene chemistry, see: Sanchez, L.; Martin, N.; Guldi, D. M. *Angew. Chem., Int. Ed.* **2005**, *44*, 5374.

(8) McClenaghan, N. D.; Absalon, C.; Bassani, D. M. *J. Am. Chem. Soc.* **2003**, *125*, 13004.

(9) (a) Huang, C. H.; McClenaghan, N. D.; Kuhn, A.; Hofstraat, J. W.; Bassani, D. M. *Org. Lett.* **2005**, *7*, 3409. (b) Huang, C. H.; McClenaghan, N. D.; Kuhn, A.; Bravic, G.; Bassani, D. M. *Tetrahedron* **2006**, *62*, 2050.

(10) McClenaghan, N. D.; Grote, Z.; Darriet, K.; Zimine, M.; Williams, R. M.; De Cola, L.; Bassani, D. M. *Org. Lett.* **2005**, *7*, 807.

(11) Korobov, M. V.; Smith, A. L. In *Fullerenes: Chemistry, Physics, and Technology*; Kadish, K. M., Ruoff, R. S., Eds.; Wiley: London, 2000.

(12) Tsunashima, R.; Noro, S. I.; Akutagawa, T.; Nakamura, T.; Kawakami, H.; Toma, K. *Chem.−Eur. J.* **2008**, *14*, 8169.

(13) Sheldrick, G. M. *Acta Crystallogr.* **2008**, *A64*, 112.

(14) Kabsch, W. *J. Appl. Crystallogr.* **1993**, *26*, 795.

Scheme 1. Synthesis of **1**[a]

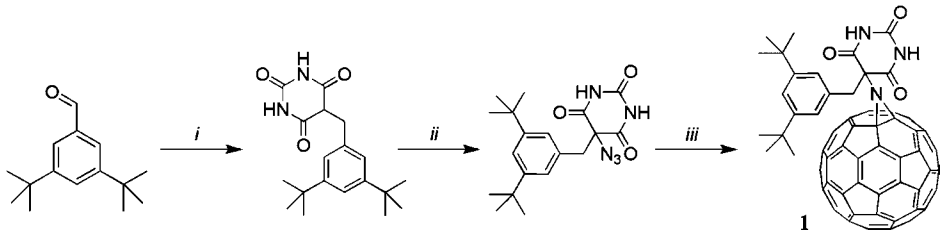

[a] Reagents and conditions: (i) barbituric acid, Pt/C, H_2, RT, 85%; (ii) NBS, DMF, then NaN_3, 92%; (iii) C_{60}, PhCl, reflux, 37%.

semiconductor analyzer system in the glovebox, where $[H_2O]$ and $[O_2] < 0.1$ ppm.

3. Results and Discussion

The synthesis of **1** is based on the addition of the corresponding azide onto C_{60},[15] as outlined in Scheme 1. Briefly, reductive alkylation of barbituric acid with 3,5-bis-*tert*-butylbenzaldehyde proceeds smoothly to afford a barbituric acid intermediate that is freely soluble even in nonpolar hydrocarbon solvents such as pentane. Bromination in the C-5 position of the barbiturate, followed by substitution with sodium azide in DMF, gives the required azido precursor. Addition to C_{60} in refluxing chlorobenzene followed by purification by column chromatography (toluene/ethyl acetate 95:5) gives **1** in 37% isolated yield. Thanks to the presence of the di-*tert*-butylbenzene solubilizing group, the solubility of **1** attains ca. 8 mg/mL in neat *o*-dichlorobenzene (*o*-DCB), and 30 mg/mL in *o*-DCB/DMSO (5%). Thermal gravimetric analysis of solid samples of **1** indicates that it is thermally stable up to ca. 100 °C.

Single crystals suitable for X-ray diffraction analysis were grown by slow diffusion of chloroform into a solution of **1** in *o*-DCB (10% DMSO). The small platelets that formed proved too thin for measurements on a conventional diffractometer, and the data was collected using synchrotron radiation on the Proxima 1 Beamline at SOLEIL. Two molecules of **1** crystallize in a triclinic (*P*-1) unit cell along with two molecules of chloroform, as shown in Figure 1. The barbituric acid is located in the plane of the fullerene cage, whereas the di-*tert*-butylbenzyl residue is pseudoaxial with respect to the C−N bond linking the barbiturate to the C_{60}. Interestingly, the relative orientation and distance of the barbituric acid residues in the crystal lattice of **1** are similar to those observed for one of the polymorphs (*C*2/*c*) of 5,5′-diethylbarbituric acid (DEB).[16] In both cases, the formation of infinite linear H-B tapes is observed because of the presence of four intermolecular H-B between barbiturates. The distance between the carbonyl oxygen and the nitrogen of a vicinal barbiturate is 2.77 Å for **1** (Figure 1) versus 2.87 Å for DEB,[16] and this similarity confirms previous results[8] suggesting that the intermolecular spacing in barbituric acid and cyanuric acid-melamine architectures is well adapted to accommodating the rigidly tethered fullerene unit.

The distribution of fullerene cages in crystals of **1** is anisotropic, contrary to what is observed for pristine C_{60} that crystallizes in a highly symmetric fcc lattice in which the fullerenes are separated by a center-to-center distance of 10.0 Å.[17] In the unit cell of **1**, this distance is 15.88 Å along the *b* and *c* axis, but only 9.95 Å along the direction of the *a* axis,

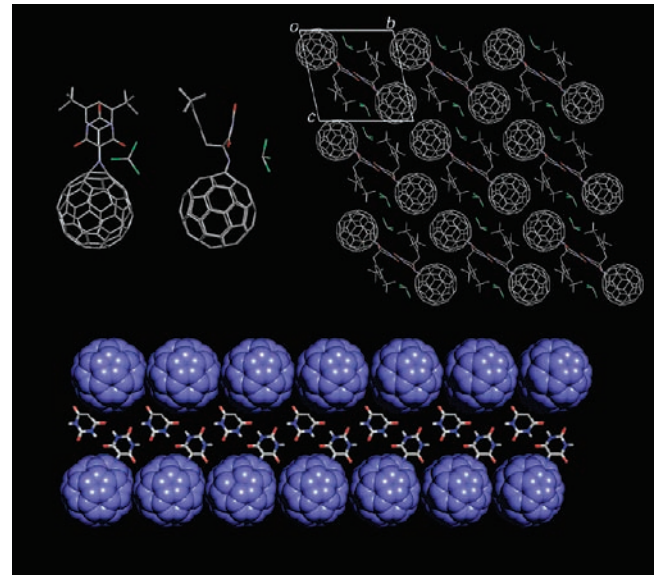

Figure 1. (Top) Solid-state crystal structure of **1** and crystal packing viewed along the *a* axis (hydrogens omitted for clarity). (Bottom) Crystal packing viewed along the *c* axis highlighting the close van der Waals contact between fullerenes in the H-B ribbon (di-*tert*-butylbenzyl groups omitted for clarity).

where the H-B ribbon draws the fullerenes into van der Waals contact (Figure 1). The H-B ribbon assembly induced by the barbituric acid residues thus leads to the formation of pairs of parallel rows of fullerenes along which charge transport is expected to be particularly efficient. In contrast, charge transport along the *b* or *c* axis would require tunneling through a barrier caused by the separation between adjacent sites (ca. 5.9 Å assuming a van der Waals radius of 10 Å for C_{60}).

The fluorescence emission from single crystals of fullerene C_{60} is bathochromically shifted with respect to what is observed in fluid solution and has been attributed to the formation of excimer-like electronically excited states.[18] Although C_{60} does not form excimers in solution, the close packing of the fullerene molecules in the solid is responsible for the augmented electronic coupling in the excited state. Halas and co-workers further showed that the structural features present in the solid-state emission spectra of C_{60} crystals could be accurately modeled using excimer theory.[18b] Fluorescence emission from crystalline solids is often polarized as a result of the alignment of the transition dipole moments. In contrast to locally excited C_{60},

(15) Prato, M.; Li, Q. C.; Wudl, F.; Lucchini, V. *J. Am. Chem. Soc.* **2002**, *115*, 1148.
(16) Craven, B. M.; Vizzini, E. A.; Rodrigues, M. M. *Acta Crystallogr., Sect. B: Struct. Sci.* **1969**, *25*, 1978.
(17) (a) Liu, S. Z.; Lu, Y. J.; Kappes, M. M.; Ibers, J. A. *Science* **1991**, *254*, 408. (b) Burgi, H. B.; Blanc, E.; Schwarzenbach, D.; Liu, S. Z.; Lu, Y. J.; Kappes, M. M.; Ibers, J. A. *Angew. Chem., Int. Ed. Engl.* **1992**, *31*, 640.
(18) (a) Sun, Y. P.; Wang, P.; Hamilton, N. B. *J. Am. Chem. Soc.* **1993**, *115*, 6378. (b) Pippenger, P. M.; Averitt, R. D.; Papanyan, V. O.; Nordlander, P.; Halas, N. J. *J. Phys. Chem.* **1996**, *100*, 2854.

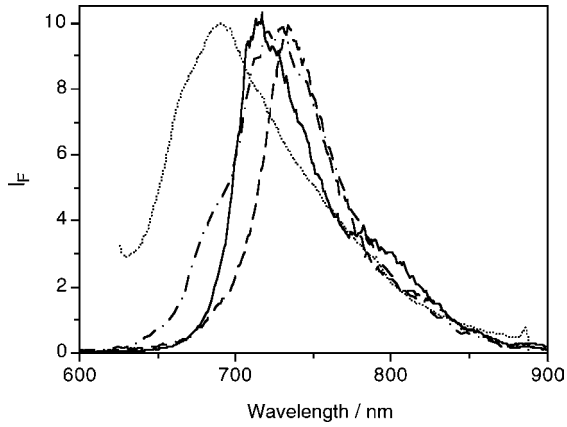

Figure 2. Comparison of the normalized fluorescence emission ($\lambda_{ex} = 385$ nm) of a single crystal of fullerene derivative **1** (—) and from a single crystal of fullerene C_{60} obtained by either vacuum sublimation (- - -) or from chloroform solution (- · -). The emission of **1** in *o*-DCB solution is also shown (· · ·, $\lambda_{ex} = 365$ nm).

whose spherical symmetry excludes polarization of the fluorescence emission, the excimer-like emission from crystalline C_{60} can be polarized because of the delocalization of the excitation energy over two (or more) fullerenes. For example, excimer (or dimer) emission from π-stacked aromatic chromophores such as pyrene[19] and perylene[20] is polarized along one of the molecular axes. However, because C_{60} crystallizes in a highly symmetric fcc lattice, we may expect excimer-like emission from C_{60} single crystals to be averaged and not polarized because each locally excited fullerene can interact with one of twelve neighboring fullerenes isotropically located within van der Waals contact. We experimentally verified this by measuring the fluorescence polarization from fullerene single crystals grown by vacuum sublimation using a confocal fluorescence microscope. The emission is very similar to that previously reported for fullerene single crystals and exhibited no detectable polarization.

The fluorescence emission from single crystals of **1** is shown in Figure 2, where it is compared to the emission in fluid solution and to the emission from single crystals of C_{60} grown by vacuum sublimation. It can be seen that the emission of **1** in the crystalline solid is considerably shifted with respect to emission from fluid solution (by 25 nm) and resembles the emission from the single crystals of pure C_{60}. We therefore attribute the emission of **1** in the crystalline phase to arise from the formation of excimer-like emitting states, analogously to what is observed for C_{60} crystals. Fluorescence polarization from single crystals of **1** was then used to investigate whether the anisotropy induced by the H-B motifs is reflected in the interfullerene electronic interactions as compared to pristine C_{60}. In contrast to single crystals of pristine C_{60}, which exhibited zero polarization, the emission from single crystals of **1** is very uniformly and highly polarized, as shown in Figure 3. The polarization (p) is defined by eq 1:

$$p = \frac{I_{\parallel} - I_{\perp}}{I_{\parallel} + I_{\perp}} \qquad (1)$$

where $I_{\parallel}$ and $I_{\perp}$ are the fluorescence emission intensity components oriented parallel and perpendicular to the polarization of the excitation beam, respectively, corrected for instrumental response except for the large numerical aperture objective

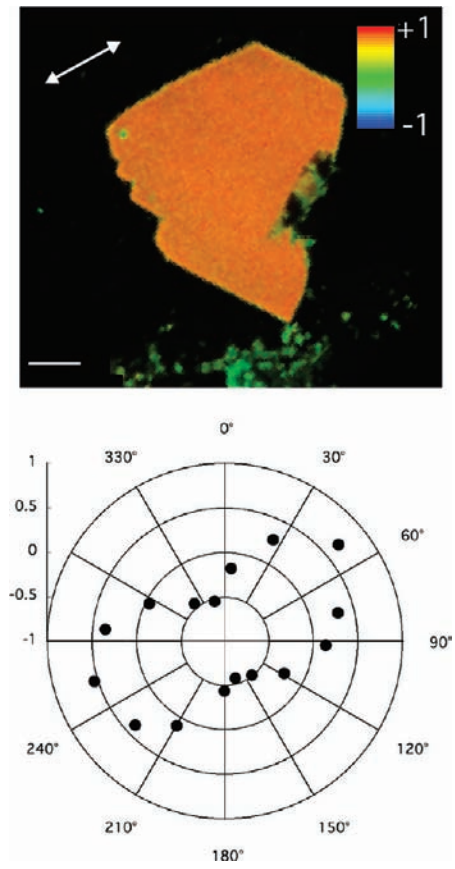

Figure 3. (Top) Confocal fluorescence polarization image of a crystal of **1** ($\lambda_{ex} = 385$ nm) color-coded according to the polarization of the emission. Double-arrow indicates direction of polarization of the excitation beam, scale bar is 10 μm. (Bottom) Polar plot of the polarization of the fluorescence emission with respect to the crystal orientation.

depolarization effects.[21] The maximum value of $p = 0.78$ obtained for a particular crystal orientation is very large yet underestimated because of the depolarization effects of the large numerical aperture objective. This clearly indicates that the excimer-like emission is highly oriented along a specific direction of the molecular crystal. Because electronic interactions in the solid are controlled by the through-space electronic coupling between adjacent fullerene cages, we deduce that the latter are likewise preferentially oriented within the crystal. Examination of the crystal structure of **1** shows that each fullerene moiety is in close contact with three other fullerenes, two of which are located on each side along the molecular H-B ribbon while the third belongs to a proximal in-plane ribbon. These pairs of adjacent fullerenes are very likely the origin of the observed orientation of the polarized emission as they are the closest in space. Further investigation showed that the polarization of the emission is independent of the orientation of the linearly polarized excitation beam relative to the crystal and that it shows a symmetric distribution of positive as well as negative p values. Such behavior suggests that the crystal's absorption is isotropic, which may be due to the high symmetry

(19) (a) Chaudhuri, M. K.; Ganguly, S. C. *J. Phys. C: Solid State Phys.* **1970**, *3*, 1791. (b) Hochstrasser, R. M.; Malliaris, A. *J. Chem. Phys.* **1965**, *42*, 2243. (c) See also: Birks, J. B. *Photophysics of Aromatic Molecules*; Wiley: New York, 1970.
(20) Fergusson, J. *J. Chem. Phys.* **1966**, *44*, 2677.
(21) (a) Bahlmann, K.; Hell, S. W. *Appl. Phys. Lett.* **2000**, *77*, 621. (b) Ha, T.; Laurence, T. A.; Chemla, D. S.; Weiss, S. *J. Phys. Chem. B* **1999**, *103*, 6839.

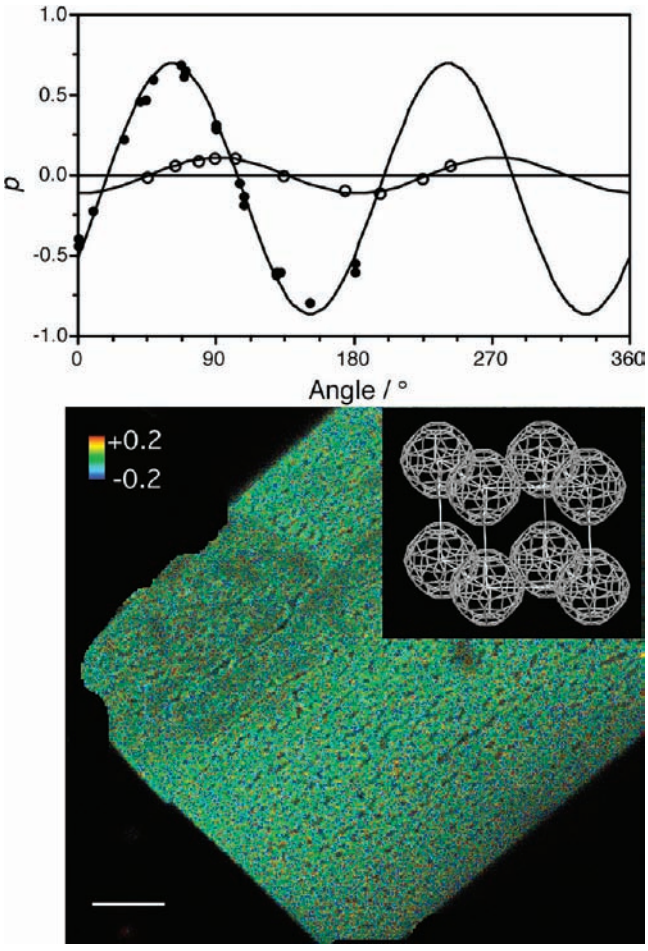

Figure 4. (Top) Comparison of polarization (p) as a function of angle of rotation (with respect to long axis of crystal) for **1** (●) and $C_{60}\cdot CHCl_3$ (○). Solid lines represent best fit through the points according to $y = A\sin(x - x_0) + c$. (Bottom) Confocal fluorescence polarization image of a crystal of $C_{60}\cdot CHCl_3$ color-coded according to the polarization of the emission (scale bar =10 μm, λ_{ex} = 385 nm, polarization of excitation beam is horizontal with respect to image). Inset: crystal packing of C_{60} cages in the molecular crystal of $C_{60}\cdot CHCl_3$ (solvent molecules are disordered and omitted for clarity).

of the fullerene chromophore and to rapid energy transfer of the initial higher energy molecular excitation to the lowest energy excimer-like emitting state.

The inclusion of solvent molecules can also lead to fullerene crystals in which the separation of the fullerenes is anisotropic, as is also the case for C_{60}-PCBM crystallized from solution.[22] Because single crystals of **1** show the inclusion of chloroform, we proceeded to investigate the effect of cocrystallized solvent on the fluorescence polarization in the solid state. To this end, crystals were grown by slow diffusion of chloroform into a toluene solution of C_{60}. The crystals thus obtained possessed the same crystal structure as that previously determined by Solovyov et al. from powder diffraction studies.[23] They are composed of hexagonally packed C_{60} planes separated by interstitial solvent molecules (space group *P*6/*mmm*; see inset in Figure 4). The fluorescence emission from these crystals also resembles that of the excimer-like emission observed from crystals of **1** or crystals of C_{60} prepared by vacuum sublimation (see Figure 2). The polarization of the emission from single crystals of **1** and $C_{60}\cdot CHCl_3$ are compared in Figure 4, where it can be seen that the maximum polarization induced by the solvent molecules alone is much lower (p = 0.11 vs. 0.78). This is indicative of a much weaker anisotropy in the interfullerene electronic interactions induced by the solvent molecules alone compared to the anisotropy induced by the H-B motifs. In line with this, we observe the fluorescence emission from $C_{60}\cdot CHCl_3$ single crystals to be only weakly polarized.

Charge carrier mobility in molecular single crystals has been found to be strongly correlated to the through-space electronic coupling between molecules, and is highest along the direction of the largest intermolecular orbital overlap integral.[24] In crystals of **1**, this would correspond to the direction of the H-B ribbon, along the *a* axis. However, although self-assembly provides a convenient route to long-range ordering in molecule-based materials, the use of ancillary fragments to induce self-organization must not interfere with the charge injection and transport processes. To date, this critical point has only been addressed for a limited number of supramolecular interactions.[25] To test whether the H-B interactions in **1** are compatible with the fabrication of *n*-type electronic devices, we investigated the charge-carrier mobility in organic field-effect transistors (OFETs) prepared using **1** and compared the results with identical devices prepared using C_{60}. Based on the anisotropic interfullerene electronic interactions revealed by the fluorescence polarization experiments, we would expect a lower value of the charge carrier mobility in the case of devices prepared from **1** with respect to C_{60}, which possesses isotropic electronic interactions that render it a good bulk semiconductor. The devices were prepared by thermal evaporation under secondary vacuum of C_{60} (device A) or **1** (device B) onto a heated SiO_2/Si (n^+-doped) substrate at 44 and 57 °C respectively. Calcium metal electrodes were then evaporated through a shadow mask to produce contacts that were 3 mm in width (W) and spaced 25 μm apart (L). Care was taken to maintain the evaporator crucible and substrate temperatures below the decomposition temperature of **1** determined from TGA measurements. Additionally, IR spectroscopy confirmed that the material deposited onto the substrate in device B possessed a spectral signature identical to that of **1**.

The I/V curves at different gate voltages for devices A and B are shown in Figure 5. In the saturation region of a plot of I_{ds} versus drain-source voltage (V_{ds}), I_{ds} follows eq 2:[26]

$$I_{ds} = \frac{WC_i}{2L}\mu(V_{gs} - V_t)^2 \qquad (2)$$

where W and L represent the channel width and length between source and drain electrodes, respectively, V_t is the threshold voltage, C_i stands for the capacitance per unit surface of the insulating layer (SiO_2 200 nm, C_i = 17.24 nF/cm^2), and μ is the charge mobility. From the linear portion of a plot of the square root of the drain-source current ($I_{ds}^{1/2}$) versus source-gate voltage (V_{gs}), the charge mobility and threshold voltage can be deduced. In the case of device A, a value of $\mu = 1.2 \times 10^{-2}$ cm^2/s V and V_t = 31 V is found, which are comparable to or somewhat lower than previously reported values of electron mobility in C_{60} OFET devices.[27] As expected, the charge mobility devices prepared from **1** (device B) is ca. 2 orders of magnitude lower, with $\mu = 1.2 \times 10^{-4}$ cm^2/s V. The lower

(22) Rispens, M. T.; Meetsma, A.; Rittberger, R.; Brabec, C. J.; Sariciftci, N. S.; Hummelen, J. C. *Chem. Commun.* **2003**, 2116.
(23) Solovyov, L. A.; Bulina, N. V.; Churilov, G. N. *Russ. Chem. Bull.* **2001**, *50*, 78.
(24) Podzorov, V. In *Organic Field-Effect Transistors*; Bao, Z., Locklin, J., Eds.; CRC Press:Boca Raton, FL, 2007.

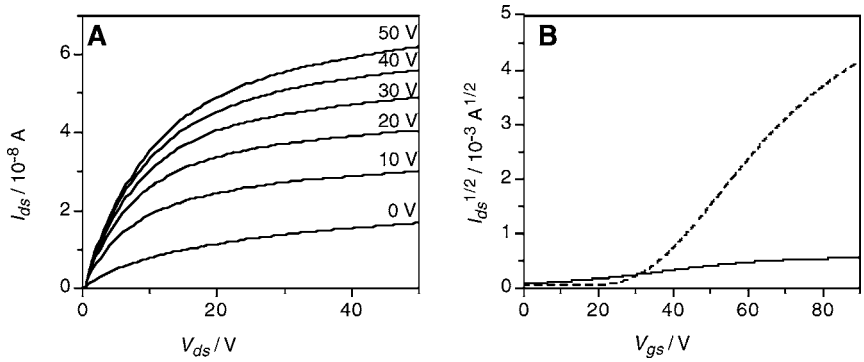

Figure 5. *I/V* characterization of OFET device B prepared using **2**. (A) I_{ds}/V_{ds} at different V_{gs}. (B) Corresponding plot of $I_{ds}^{1/2}$ at saturation versus V_{gs} for **1** (device B, solid line) and for C_{60} (device A, dashed line).

threshold voltage, $V_t \approx 3$ V,[28] suggests better matching of the energy level of the work function of the Ca electrode (2.87 eV) with the electron affinity of **1** versus C_{60}, which is expected to facilitate charge injection.[29]

It has been previously shown that charge mobility in OFET devices is strongly influenced by grain size,[30] and this may also contribute to the difference in μ observed between the two devices. For example, in pentacene OFETs, which possess a similar granular morphology as devices A and B, the charge carrier mobility is found to decrease rapidly with decreasing grain size, especially for grain sizes <2 μm.[31] Di Carlo et al. modeled the device properties and proposed that the existence of barriers between grains is mainly responsible for the decrease in mobility in devices with smaller grains.[32]

The difference in the surface morphology between devices A and B was investigated by AFM (Figure 6). In both cases, the surface is granular, with grains averaging ca. 80 and 40 nm in device A and B, respectively. The smaller grain size in device B compared to A is somewhat surprising, considering that it was prepared at a slightly higher substrate temperature (57 vs 44 °C) and that higher substrate temperatures favor the formation of larger grains.[33] During the thermal evaporation process,

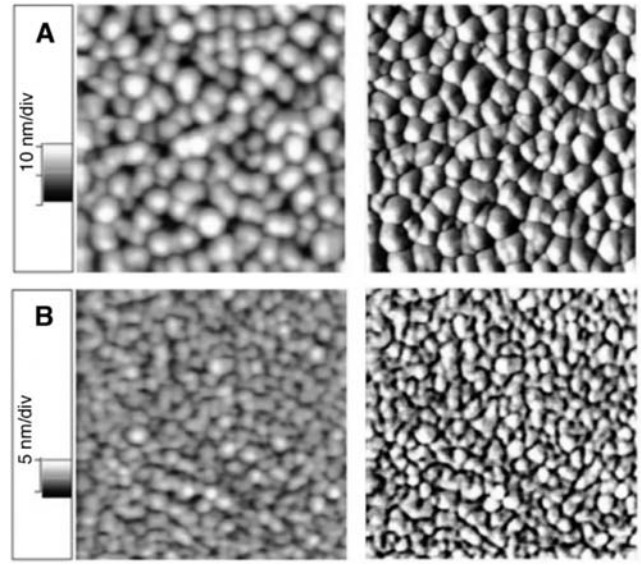

Figure 6. AFM topography (left) and phase (right) images of devices A and B prepared by thermal evaporation of C_{60} or **1**, respectively. Images are 1 μm × 1 μm.

individual molecules are deposited on the substrate and dissipate part of their excess thermal energy as translation motion on the surface. Heating the substrate can favor this mobility, leading to the growth of larger domains. The smaller grains obtained from the thermal depostition of **1** may therefore indicate that it possesses a lower surface mobility compared to C_{60}, which may be due to H-B interactions between molecules on the surface. Since the thickness of the active layer in the devices (40−100 nm) is of the same order of magnitude as the size of the grains observed by AFM, it is likely that the granular morphology extends into the bulk of the active layer, reaching the SiO_2/semiconductor interface.

4. Conclusion

We have successfully developed a fullerene derivative allying the presence of multiple H-B sites and solubility in organic media. Its solid-state crystal structure bears great similarity to that of the barbituric acid H-B molecular recognition unit, indicating that it is the latter that directs association in the solid as opposed to aggregation of the C_{60} moieties. The barbituric acid residues direct the self-assembly of **1** into infinite H-B tapes oriented along one of the crystal axis, which then stack along the $b-c$ direction. One may therefore expect strong anisotropy in the electrical conductivity of the crystals of **1**, which would

(25) Fullerene derivatives possessing H-B substituents have been used in solution-based devices. For examples, see refs 6e, 9 and Liu, Y.; Xiao, S.; Li, H.; Li, Y.; Liu, H.; Lu, F.; Zhuang, J.; Zhu, D. *J. Phys. Chem. B* **2004**, *108*, 6256. For an example of a H-B fullerene-porphyrin photoelectrochemical device, see: Kira, A.; Tanaka, M.; Umeyama, T.; Matano, Y.; Yoshimoto, N.; Zhang, Y.; Ye, S.; Lehtivuori, H.; Tkachenko, N. V.; Lemmetyinen, H.; Imahori, H. *J. Phys Chem. C* **2007**, *111*, 13618. Wessendorf, F.; Gnichwitz, J. F.; Sarova, G. H.; Hager, K.; Hartnagel, U.; Guldi, D. M.; Hirsch, A. *J. Am. Chem. Soc.* **2007**, *129*, 16057. An OFET device based on a fullerene-amide dendron has been reported by Kusai:Kusai, H.; Nagano, T.; Imai, K.; Kubozono, Y.; Sako, Y.; Takaguchi, Y.; Fujiwara, A.; Akima, N.; Iwasa, Y.; Hino, S. *Appl. Phys. Lett.* **2006**, *88*, 173509.
(26) Horowitz, G. *Adv. Mater.* **1998**, *10*, 365.
(27) Haddon, R. C.; Perel, A. S.; Morris, R. C.; Palstra, T. T. M.; Hebard, A. F.; Fleming, R. M. *Appl. Phys. Lett.* **1995**, *67*, 121.
(28) The value of V_t is difficult to determine with precision because of the low charge carrier mobility of **1**.
(29) The electron affinity of **1** is expected to be ca. 0.2 eV higher than that of C_{60} on the basis of the difference of the onset of their reduction potentials.
(30) Nakamura, M.; Ohguri, H.; Goto, N.; Tomii, H.; Xu, M. S.; Miyamoto, T.; Matsubara, R.; Ohashi, N.; Sakai, M.; Kudo, K. *Appl. Phys. A: Mater. Sci. Process.* **2009**, *95*, 73.
(31) (a) Chen, J. H.; Tee, C. K.; Shtein, M.; Anthony, J.; Martin, D. C. *J. Appl. Phys.* **2008**, *103*, 114513. (b) Cho, S. M.; Han, S. H.; Kim, J. H.; Janga, J.; Oh, M. H. *Appl. Phys. Lett.* **2006**, *88*, 071106.
(32) Di Carlo, A.; Piacenza, F.; Bolognesi, A.; Stadlober, B.; Maresch, H. *Appl. Phys. Lett.* **2005**, *86*.
(33) Pratontep, S.; Nüesch, F.; Zuppiroli, L.; Brinkmann, M. *Phys. Rev. B: Condens. Matter* **2005**, *72*, 085211.

also be reflected in lowered bulk charge carrier mobility with respect to C_{60} if nanocrystalline domains are formed during the deposition process. The use of H-B interactions therefore complements other approaches to obtaining fullerene nanostructures of controlled dimensionality that rely on nondirective hydrophobic forces during deposition from fluid solutions.[12,34,35] Fluorescence polarization of fullerene emission in the solid was found to be a useful technique to characterize anisotropy in the electronic interactions between adjacent fullerenes that may find further applicability. The strongly polarized fluorescence originating from fullerene excimer-like emitting states in single crystals of **1** is in agreement with the ordered orientation of the fullerenes in the solid. Concerning the use of H-B fullerenes for the fabrication of electronic devices, we find that the bulk charge carrier mobility in OFET devices prepared using **1** is ca. 2 orders of magnitude lower than that measured for C_{60}. We attribute this to the lower dimensionality of **1** as a conductor, although variations in grain size in the active layer of the OFET devices may also contribute. This indicates that, despite the greater sensitivity of *n*-type versus *p*-type organic semiconductors, the presence of imide H-B units is not deleterious to charge transport. The fabrication of extended linear fullerene polymers through H-B self-assembly is especially interesting for the construction of molecular-level devices in which the molecular units are designed to self-organize into the principal components, e.g., wires, junctions, etc. Investigations of the formation and electronic properties of such nanowires on semiconducting and insulating surfaces are currently in progress.

Acknowledgment. We warmly thank Dr. Pierre Legrand at SOLEIL for beamtime and his help during data collection on PROXIMA1 Beamline and Mrs. O. Babot for the TGA measurements. Financial support for this work was provided by the Advanced Materials in Aquitaine foundation, the Agence Nationale de la Recherche (ANR-08-BLAN-016101), and the Région Aquitaine.

Supporting Information Available: General methods and full experimental details for the synthesis of **1**, fluorescence lifetime image of a single crystal of C_{60} obtained by vacuum-sublimation and histogram of emission polarization, *I*/*V* characterization of device A, thermal gravimetric analysis, IR spectra, and crystal structure of **1** in CIF format. This material is available free of charge via the Internet at http://pubs.acs.org.

JA104750F

(34) Piot, L.; Silly, F.; Tortech, L.; Nicolas, Y.; Blanchard, P.; Roncali, J.; Fichou, D. *J. Am. Chem. Soc.* **2009**, *131*, 12864.
(35) Geng, J. F.; Zhou, W. Z.; Skelton, P.; Yue, W. B.; Kinloch, I. A.; Windle, A. H.; Johnson, B. F. G. *J. Am. Chem. Soc.* **2008**, *130*, 2527.